

## RESEARCH ARTICLE

# Intra-colony spatial variance of oxyregulation and hypoxic thresholds for key *Acropora* coral species

Nicole J. Dilernia<sup>1</sup>  | Stephen Woodcock<sup>2</sup>  | Emma F. Camp<sup>1</sup>  | David J. Hughes<sup>3</sup>  | Michael Kühl<sup>4</sup>  | David J. Suggett<sup>1,5</sup> 

<sup>1</sup>Climate Change Cluster, University of Technology Sydney (UTS), Ultimo, New South Wales, Australia

<sup>2</sup>School of Mathematical and Physical Sciences, University of Technology Sydney (UTS), Ultimo, New South Wales, Australia

<sup>3</sup>National Sea Simulator, Australian Institute of Marine Science (AIMS), Townsville, Queensland, Australia

<sup>4</sup>Department of Biology, Marine Biological Section, University of Copenhagen, Helsingør, Denmark

<sup>5</sup>KAUST Reefscape Restoration Initiative (KRRRI) and Red Sea Research Center (RSRC), King Abdullah University of Science and Technology, Thuwal, Saudi Arabia

## Correspondence

Nicole J. Dilernia, Climate Change Cluster, University of Technology Sydney (UTS), Ultimo 2007, NSW, Australia.  
Email: [nicole.j.dilernia@student.uts.edu.au](mailto:nicole.j.dilernia@student.uts.edu.au)

## Funding information

Australian Research Council Discovery Project, Grant/Award Number: DP230100210; Australian Government Research Training Program Scholarship

## Abstract

Oxygen (O<sub>2</sub>) availability is essential for healthy coral reef functioning, yet how continued loss of dissolved O<sub>2</sub> via ocean deoxygenation impacts performance of reef building corals remains unclear. Here, we examine how intra-colony spatial geometry of important Great Barrier Reef (GBR) coral species *Acropora* may influence variation in hypoxic thresholds for upregulation, to better understand capacity to tolerate future reductions in O<sub>2</sub> availability. We first evaluate the application of more streamlined models used to parameterise Hypoxia Response Curve data, models that have been used historically to identify variable oxyregulatory capacity. Using closed-system respirometry to analyse O<sub>2</sub> drawdown rate, we show that a two-parameter model returns similar outputs as previous 12th-order models for descriptive statistics such as the average oxyregulation capacity (T<sub>pos</sub>) and the ambient O<sub>2</sub> level at which the coral exerts maximum regulation effort (P<sub>cmax</sub>), for diverse *Acropora* species. Following an experiment to evaluate whether stress induced by coral fragmentation for respirometry affected O<sub>2</sub> drawdown rate, we subsequently identify differences in hypoxic response for the interior and exterior colony locations for the species *Acropora abrotanoides*, *Acropora cf. microphthalmma* and *Acropora elseyi*. Average regulation capacity across species was greater (0.78–1.03 ± SE 0.08) at the colony interior compared with exterior (0.60–0.85 ± SE 0.08). Moreover, P<sub>cmax</sub> occurred at relatively low pO<sub>2</sub> of <30% (±1.24; SE) air saturation for all species, across the colony. When compared against ambient O<sub>2</sub> availability, these factors corresponded to differences in mean intra-colony oxyregulation, suggesting that lower variation in dissolved O<sub>2</sub> corresponds with higher capacity for oxyregulation. Collectively, our data show that intra-colony spatial variation affects coral oxyregulation hypoxic thresholds, potentially driving differences in *Acropora* oxyregulatory capacity.

## KEYWORDS

Coral oxyregulator, Coral reefs, Climate change, Hypoxic tolerance, Hypoxia Response Curves, Ocean deoxygenation

This is an open access article under the terms of the [Creative Commons Attribution](https://creativecommons.org/licenses/by/4.0/) License, which permits use, distribution and reproduction in any medium, provided the original work is properly cited.

© 2024 The Authors. *Ecology and Evolution* published by John Wiley & Sons Ltd.

## TAXONOMY CLASSIFICATION

Evolutionary ecology

### 1 | INTRODUCTION

Oxygen (O<sub>2</sub>) availability in marine systems (Breitburg et al., 2018), including coral reefs (Altieri et al., 2017; Hughes et al., 2020), is deteriorating under intensifying anthropogenic pressures. Loss of soluble O<sub>2</sub> via ocean warming (Keeling et al., 2010; Sampaio et al., 2021) and increased biological O<sub>2</sub> demand under reduced water quality (Keeling et al., 2010; Levin & Breitburg, 2015) can lead to deoxygenation—an often overlooked and relatively unstudied stressor on coral reefs (Hughes et al., 2020; Nelson & Altieri, 2019; Sampaio et al., 2021). Future global ocean projections under climate change predict deoxygenation of up to 7% by 2100 (Alderdice et al., 2021; Breitburg et al., 2018; Keeling et al., 2010; Pezner et al., 2023), and low O<sub>2</sub> stress termed ‘hypoxia’ (<2 mg O<sub>2</sub> L<sup>-1</sup> or ~25% air sat) thus poses an increasing threat to coral reef health and survival (Altieri et al., 2017; Diaz & Rosenberg, 1995; Klein et al., 2020; Steckbauer et al., 2011; Vaquer-Sunyer & Duarte, 2008). Whilst the full capacity for coral survival under increasing hypoxia remains unknown (Hughes, Alexander, et al., 2022; Johnson, Scott, et al., 2021), many marine organisms are being pushed to their lower limits for healthy metabolic functioning (Diaz & Rosenberg, 1995; Steckbauer et al., 2020; Vaquer-Sunyer & Duarte, 2008), including cnidarians adapting to reduce metabolic rates (Rutherford & Thuesen, 2005; Vaquer-Sunyer & Duarte, 2008), or relying on alternative sources of energy to survive under sustained hypoxic conditions (Linsmayer et al., 2020; Murphy & Richmond, 2016).

Hypoxia response curves (HRCs) are commonly employed to assess the performance of aquatic organisms (Carey et al., 2013; Cobbs & Alexander, 2018; Tremblay et al., 2020), and more recently corals (Hughes, Alexander, et al., 2022), under increasing hypoxia. Although hypoxic tolerance can be examined using various time versus dose-dependent approaches (Alderdice et al., 2021; Alva García et al., 2022; Johnson, Scott, et al., 2021), the use of closed-system respirometry for quantifying hypoxic response (or ‘performance’) curves—much like rapid thermal performance curves (e.g., Aichelman et al., 2019; Dileria et al., 2023)—enable relatively high throughput. Hypoxia response curves display patterns of O<sub>2</sub> consumption, that is, respiration (VO<sub>2</sub>, mg h<sup>-1</sup>) over time, against ambient levels of O<sub>2</sub> (pO<sub>2</sub>, % air saturation) (Hughes, Alexander, et al., 2022). Historically, many organisms such as cnidarians (including corals) were assumed to exhibit respiration rates that varied in direct proportion to their ambient O<sub>2</sub> level (Seibel et al., 2021; Shick, 1990; Ultsch & Regan, 2019)—an attribute known as oxyconformity (Hughes et al., 2020; Hughes, Alexander, et al., 2022). However, HRC measurements recently revealed that corals can in fact oxyregulate, controlling their respiration capacity irrespective of the ambient O<sub>2</sub> (Hughes, Alexander, et al., 2022). Whilst Hughes,

Alexander, et al. (2022) only studied a handful of coral taxa from the Great Barrier Reef (GBR) and aquaria, the study resolved hypoxic thresholds for oxyregulation for the first time for key coral reef-forming species, extending beyond other observations that had captured time-dependent limits of survival to specific low O<sub>2</sub> concentrations (e.g., Alderdice et al., 2021; Johnson, Scott, et al., 2021; Johnson, Swaminathan, et al., 2021).

Previous studies have utilised a range of methods to parameterise the change in O<sub>2</sub> consumption as a function of declining O<sub>2</sub> availability based on HRC analysis (e.g., Rutherford & Thuesen, 2005; Ultsch & Regan, 2019; Zhang & Farrell, 2022). This includes the ‘regulation profile’ method proposed by Cobbs and Alexander (2018), which derives broad descriptive statistics of an organisms oxyregulatory capacity. For example, the extent of total positive regulation (T<sub>pos</sub>, relative units)—or the ‘average’ regulation beyond strict oxyconformity—and the minimum and maximum regulation capacity (P<sub>min</sub>/P<sub>max</sub>), that is, the pO<sub>2</sub> level (% air saturation) at which taxa exert minimum/maximum regulation effort (Cobbs & Alexander, 2018). The P<sub>max</sub> parameter has also been proposed as an extension of the well-known critical O<sub>2</sub> tension parameter, P<sub>crit</sub> (Cobbs & Alexander, 2018) or P<sub>crit-max</sub> (Seibel et al., 2021), which define the lowest pO<sub>2</sub> level (% air sat) at which an organism can maintain a constant VO<sub>2</sub> (Pontes et al., 2023; Regan et al., 2019; Seibel et al., 2021), that is, the maximum oxyregulation capacity. In this way, P<sub>max</sub> describes the hypoxic threshold for upregulation, where regulation capacity cannot increase past this point. Recent work applying HRCs showed that corals can exhibit moderate capacity for oxyregulation, with substantial variability among coral taxa, and interestingly finding greatest differences in total positive regulation (T<sub>pos</sub>) between species of the same genus, e.g., *Pocillopora damicornis* displaying the lowest average total positive regulation (0.41), compared with *P. acuta* (2.42) (Hughes, Alexander, et al., 2022).

Tropical coral reefs span highly dynamic O<sub>2</sub> environments, from shallow waters of tidal pools and fringing reefs that regularly endure natural O<sub>2</sub> depletion, to much deeper reefs (>100 m) threatened by oxygen minimum zones (OMZs; Giomi et al., 2019; Hughes et al., 2020; Nelson & Altieri, 2019). The limited amount of data in the literature suggest that coral taxa exhibit a broad range of O<sub>2</sub> tolerance and hypoxic thresholds (Alva García et al., 2022; Johnson, Scott, et al., 2021; Johnson, Swaminathan, et al., 2021; Pontes et al., 2023) and regulatory dynamics (Alderdice et al., 2021; Hughes, Alexander, et al., 2022). Yet, it is unclear how these differences reflect inherent tolerance to deoxygenation exposure for any given individual (Deleja et al., 2022) and whether hypoxic thresholds are fine-tuned by acclimatisation to different environments remains unknown. That said, for corals changes in flow are likely critical to local O<sub>2</sub> availability whereby colony growth form

can define the local flow regime (Hossain & Staples, 2020; Jimenez et al., 2011). Edge environments of corals, in comparison with the centre of colonies, have been found to experience higher flow (Hossain & Staples, 2020), which in turn shapes colony level variance of bacterial communities (Fifer et al., 2022). Given that HRCs in the past typically do not employ standards for acquisition of coral samples, it is plausible that differences in colony sample location—and particularly for complex branching morphologies—will experience very different  $O_2$  dynamics inside than out—however, whether this results in different hypoxic thresholds for oxyregulation remains untested.

Here we use HRC analysis to test the hypothesis that intra-colony variation in hypoxic tolerance exists for *Acropora* species common on the GBR, with interior branches exhibiting inherently lower thresholds for hypoxia (and an increased oxyregulatory capacity) compared to 'exterior' branches of the same colony. First, we conducted an experiment to analyse whether the process of sampling (i.e., removing fragments) induces stress that may alter  $O_2$  physiological parameterisation. Second, we aimed to advance current HRC model fitting—and address unresolved key methodological steps to improve confidence in HRC parameter retrieval. To do this, we compared oxyregulatory descriptive statistics extracted from models with multiple-polynomial degrees (up to 12th order) (Hughes, Alexander, et al., 2022), to the most parsimonious model (i.e., simplest model with fewest parameters), since the biological rationale for the amount of inflexion points necessary in fitting HRCs remains undefined as are the specific biological mechanisms employed by corals during the process of oxyregulation (Hughes, Alexander, et al., 2022). To address these various questions, we examined a range of *Acropora* species—*A. hyacinthus*, *A. intermedia*, and *A. kenti* (formerly *A. tenuis*, Bridge et al., 2023)—as originally sampled by Hughes, Alexander, et al. (2022), as well as *A. loripes*, *A. abrotanoides*, *A. cf. microphthalma* and *A. elseyi*, thereby adding insight into inherent inter-species and intra-colony variance in oxyregulatory hypoxic thresholds for this key reef-building genus. Results from this work highlight important considerations for future sampling of corals, including any potential spatial variation in the future susceptibility of coral colonies to deoxygenation events, to further resolve their variable  $O_2$  physiologies.

## 2 | MATERIALS AND METHODS

### 2.1 | Coral fragment collection

Coral fragments of ~5–10 cm length were collected using wire cutters from select *Acropora* colonies of branching morphology (Table 1) from Opal Reef (GBR, Australia; 16.220°S, 145.885°E), for two experiments. All fieldwork and collections were carried out from the 2nd to the 17th of February 2022, under Permit No. G20/43740.1 (Great Barrier Reef Marine Park Authority). We note that the laboratory set-up allowed for a maximum of six coral fragments per

incubation; therefore, sampling was carried out over multiple days, as further described below.

#### 2.1.1 | Experiment 1: Fragmentation effects

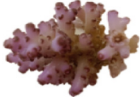


We first tested for any potential stress induced by physically fragmenting coral, and how recovery time could potentially influence  $O_2$  drawdown during closed system respirometry. For this, a total of six colonies of *A. loripes*—of varying colour and similar colony size (<1 m) and depth (~4 m)—were selected at Rayban, Opal Reef (Table 1; Lines 1a and 1b) and marked with flagging tape. From each colony, one fragment was removed and immediately secured back onto the reef substrate next to its parent colony location using a CoralClip® (Suggett et al., 2020). After 7-day postfragmentation recovery, we returned to the same reef location and collected fragments from the CoralClip® ( $n=3$  fragments), on the 8th of February 2022, and again on the 9th of February 2022, as well as taking new fragments from each of the same six colonies ( $n=3$  fragments) on both days (Table 1). All samples ( $n=6$  clipped,  $n=6$  fresh, total) were taken from parent colonies at least 5–10 m apart.

#### 2.1.2 | Experiment 2: Interior versus exterior colony variance

To determine whether and how sampling location could potentially affect the  $O_2$  physiology of the coral, three *Acropora* species (*A. abrotanoides*, *A. cf. microphthalma*, and *A. elseyi*) from three colonies (one colony per species) at varying water depth (2–4 m) were selected (Table 1; Lines 2–4). Replicate fragments were removed from each chosen colony, first from the thicket interior ( $n=3$ ), and then the exterior open branches ( $n=3$ ), twice over two sampling days (see Table 1 for full sampling schedule).

For both experiments, coral fragments were collected by SCUBA and placed into Ziplock bags for immediate transport to the surface support vessel. Samples were then immediately transported (~60 min) back to a temporary laboratory setup on shore in a 40-L portable cooler box filled with fresh seawater collected at the site of origin. During transportation, the cooler box lid was left open, corals were shaded from direct sunlight using a black mesh cover, and temperature was monitored regularly using a floating glass thermometer (unbranded). Seawater was constantly aerated using two air-stones connected to battery-operated air pumps (Aqua One Battery Air 250). Prior to reaching shore (after ~30 min of travel), 90% of the total seawater in the cooler box was exchanged for fresh seawater (also collected from site)—without exposing the coral fragments to air—before being immediately transported from the boat for respirometry assessment. Dissolved oxygen (DO) levels of the seawater were tested again immediately after transportation from the boat to the onshore laboratory using a robust oxygen probe (OXROB10-SUB; PyroScience, Germany) connected to an oxygen data metre (FireSting-O2; PyroScience GmbH, Germany)—remaining above 87% air sat.

TABLE 1 Properties of *Acropora* colonies with different branching morphology sampled in the field at Opal Reef (GBR, Australia) from the 5th to the 17th of February 2022.

Fragment image	Coral species	Site at opal reef	No. colonies	Sample size	Date sampled	Colony depth (m)	Colony size (m)
	1a	Rayban	6	n = 6 clipped with CoralClip®	Feb 2, 2022	3.5–4	0.3–1
	1b		6	n = 3 clipped, 3 fresh n = 3 clipped, 3 fresh	Feb 8, 2022 Feb 9, 2022	3.5–4	
	2	Mojo	1	O <sub>2</sub> Logger deployed n = 3 interior, 3 exterior n = 3 interior, 3 exterior	Feb 5, 2022 Feb 6, 2022 Feb 7, 2022	2	0.95
	3	Mojo	1	O <sub>2</sub> Logger deployed n = 3 interior, 3 exterior n = 3 interior, 3 exterior	Feb 7, 2022	3	1.2
					Feb 10, 2022 Feb 11, 2022		
	4	Rayban	1	O <sub>2</sub> Logger deployed n = 3 interior, 3 exterior n = 3 interior, 3 exterior	Feb 12, 2022 Feb 12, 2022 Feb 13, 2022	3.5	1.5

Note: NB: total fragment sample size for interior/exterior of each colony was  $n = 6$ .

## 2.2 | Hypoxia response curve (HRC) measurements

Following transportation from Opal Reef (as described in Section 2.1) and prior to incubation, each individual coral fragment was inspected and carefully cleaned of any additional debris (e.g., detachable algae and crabs) using forceps and a soft-bristled toothbrush (as per Hughes, Alexander, et al., 2022), before being placed in individual respirometry chambers filled with fresh, aerated seawater from the sampling site. Chambers were sealable glass jars (400 mL), each with a hinged wire clasp gas-tight lid, containing a plastic mesh-platform upon which the fragment was placed, allowing space beneath for free rotation of a 30 × 7 mm magnetic stirring bar (PTFE, ROWE Scientific Pty Ltd). Each chamber was fitted with an optical O<sub>2</sub> sensor spot (OXSP5; PyroScience) fixed on the inside of the glass with silicon glue (SPGLUE, Elastosil E43, WACKER, US), for contactless sensor readout via a fibre-optic O<sub>2</sub> probe (SPFIB-BARE; PyroScience) mounted on the transparent chamber. Each probe was connected to a fibre-optic O<sub>2</sub> metre (FireSting-O2, PyroScience GmbH) to continuously monitor the dissolved O<sub>2</sub> content (% air sat) of the chamber. All O<sub>2</sub> sensor spots were calibrated against 100% air-saturated seawater and a 0% O<sub>2</sub> solution prepared by adding sodium sulphite (Na<sub>2</sub>SO<sub>3</sub>) to de-mineralised water, prior to incubations.

Corals were acclimated for at least 60 min in their individual chambers, which were left unsealed and constantly aerated by an air-stone connected to an air pump (Marina 200 Aquarium Air Pump), ensuring DO was maintained at >90% of air saturation during this time as per Hughes, Alexander, et al. (2022). Chambers were three-quarters submerged in a water bath maintained at 27 ± 0.5°C (corresponding to in situ temperature at the time of sample collection) by a heating immersion circulator (EH, JULABO, Julabo USA, Inc.), and positioned on top of a multi-station stirring plate (iStir HP 10M, Neutution Technologies Pty Ltd) to magnetically stir the individual stir bars (~500 rpm). Following acclimation, at least 90% of the seawater in each individual chamber was exchanged, temperature-adjusted to 27°C by a 150 W bar heater (Aqua One Submersible Glass Heater, 230V/50Hz) and aerated with a water pump (Aqua Pro Tabeltop Feature Pump, AP200LV). To avoid exposing the coral fragment to air during this exchange, one end of silicon tubing was connected to the water pump in the fresh seawater, with the other end positioned inside the bottom of the chamber to turnover old with fresh seawater. The chambers were then sealed with the wire clasp gas-tight lid whilst completely submerged, ensuring no trapping of air bubbles inside.

Closed-system respirometry was used to measure HRCs (Hughes, Alexander, et al., 2022; Killen et al., 2021). The closed chambers were fully submerged in the heated water bath during incubation, with the entire bath surrounded by purpose cut black-out cloth and boards to emulate dark conditions of the natural diel cycle (Alderdice et al., 2021). Starting with DO levels as close to 100% of air saturation as possible, drawdown rates of the ambient O<sub>2</sub> (pO<sub>2</sub>) were monitored as coral fragments respired. Dissolved O<sub>2</sub> content was measured every 60 s, and incubations were terminated after

reaching 0% air saturation (or at least <2% air sat during time limitations), over a period of ~6–12 h. Ancillary microbial respiration in the seawater was also measured via supplementary control incubations containing seawater only from the corresponding coral sampling site. In addition, volumes of seawater displacement were determined to normalise individual fragment size to chamber capacity. O<sub>2</sub> consumption rates from the seawater controls and the volumes displaced by the corals were subtracted from the rates measured of the individual corresponding coral fragments. Mean O<sub>2</sub> consumption rates for each coral fragment were then calculated, per hour (VO<sub>2</sub>, mg h<sup>-1</sup>).

## 2.3 | In situ O<sub>2</sub> logger deployment

Prior to each sampling event (as described above in Section 2.1), two optical O<sub>2</sub> sensor data loggers (AquapHOx-L-O2; PyroScience GmbH) were deployed to measure the corresponding ambient O<sub>2</sub> and temperature (with a logging interval set at 60 s) in the *Acropora* colonies, from where the interior versus exterior coral samples were taken (Table 1; Lines 2–4). Due to constraints surrounding boat scheduling, the O<sub>2</sub> loggers were deployed 1 day prior to the first coral fragment collection in *A. abrotanoides* and *A. elseyi*, and 1.5 days prior to first sampling in *A. cf. microphthalmma*. A robust O<sub>2</sub> probe (OXROB10-SUB; PyroScience) was attached to the SUB-connector optical port of each data logger, and the tips of these sensors were positioned in the same areas of the colonies from where the fragments were taken for respirometry assessment, that is, (1) in the interior thicket, and (2) in the exterior open branches. The sensors were cable-tied in position, deployed for 2–3 days at a time, measuring DO (mg O<sub>2</sub> L<sup>-1</sup>) at 60-s intervals. The main bodies of the loggers were secured to lead diving weights and positioned on the reef substrate next to the chosen colony, additionally measuring the ambient seawater temperature (°C). The AquapHOx-L-O2 loggers were calibrated against 100% air-saturated seawater and a 0% O<sub>2</sub> solution prior to deployment.

## 2.4 | Statistical analysis

All statistical analyses were carried out in RStudio version 4.1.0, Build 446 (R Core Team, 2021) with base packages: knitr v. 1.33 (Xie, 2014, 2015, 2021), rmarkdown v. 2.20 (Allaire et al., 2023; Xie et al., 2018, 2020), and tidyverse v. 2.0.0 (Wickham et al., 2019).

### 2.4.1 | Hypoxia response curve modelling

An initial assessment of model fit via Akaike Information Criterion (AIC) for oxyregulation parameter extraction (e.g., T<sub>pos</sub>, see Figure 1a) was made using data previously collected and analysed by Hughes, Alexander, et al. (2022) using the 'regulation profile' method (Cobbs & Alexander, 2018). This ensured data retrieved

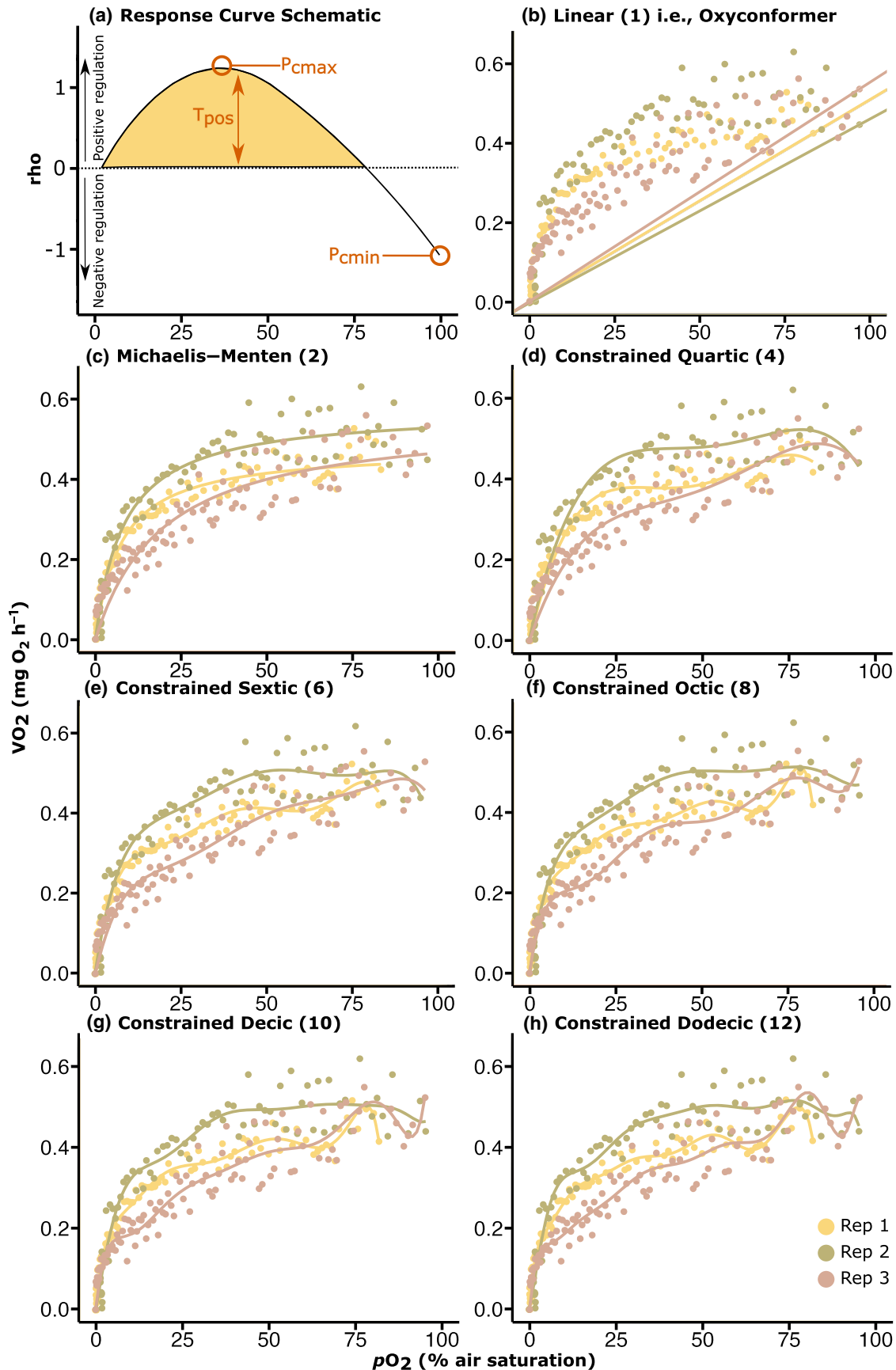


**FIGURE 1** (a) Schematic diagram outlining points of extraction for hypoxia response curve (HRC) parameters ( $T_{pos}$ ,  $P_{cmax}$  and  $P_{cmin}$ ) using the  $\rho(pO_2)$  equation (Equation 1), in addition to (b–h) models of varying polynomial degrees (1–12th order) fit to replicates of HRC data sets of model species *Acropora kenti* ( $n=3$ ) (from Hughes, Alexander, et al., 2022). Replicates indicated by colour, and individual model fits (per rep) by lines.



from our study was comparable to that from species of *Acropora* previously analysed. Models of varying polynomial orders—increasing from a linear (1st degree) through to a constrained dodecic (12th degree) polynomial—were fit to three sets of *Acropora* HRC data ( $n=3$ )—*A. hyacinthus*, *A. intermedia* and *A. kenti*—previously collected via the same respirometry assay method as for our current study (Hughes, Alexander, et al., 2022). Note that as per (Hughes, Alexander, et al., 2022), an AIC selection of a 1-parameter linear model fit would suggest strict oxyconformity, that is, no oxyregulation being performed by the coral (similar to ‘Model S1’ as described in Cobbs and Alexander (2018)), whilst any other model selected above a first-degree polynomial indicates some capacity for oxyregulation. All model fits and plots prepared here used RStudio installed packages ‘drc’ v. 3.0.1 (Ritz et al., 2015) and ‘ggplot2’ (Wickham, 2016).

Following this, oxyregulatory descriptive statistics ( $T_{\text{pos}}$ ,  $P_{\text{cmax}}$  and  $P_{\text{cmin}}$ ) were extracted from the parameter estimates of the above model fits using the regulation function  $\rho(\text{pO}_2)$  (Cobbs & Alexander, 2018):

$$\rho(\text{PO}_2) = \frac{f(\text{PO}_2)}{\text{PO}_2} - f'(\text{PO}_2) \quad (1)$$

Significant differences between the extracted parameters from each HRC fit were tested using a series of independent sample *t*-tests using RStudio installed package ‘rstatix’ version 0.7.2 (Kassambara, 2023b). Note that the units for  $T_{\text{pos}}$  are ‘relative’, whilst units for  $P_{\text{cmax}}$  and  $P_{\text{cmin}}$  are given as  $\text{O}_2$  concentrations in units of % air saturation. All data for analyses were checked for normality using the Shapiro–Wilk test, and distribution via Q–Q plots, whilst homogeneity of variance was checked using Levene’s test. We used a correlation and regression analysis, using RStudio installed packages ‘car’ (Fox & Weisberg, 2019), ‘ggpubr’ (Kassambara, 2023a), and ‘ggplot2’ (Wickham, 2016), to examine the relationship between the parameters extracted from the original HRCs of *A. hyacinthus*, *A. intermedia*, and *A. kenti* as per (Hughes, Alexander, et al., 2022) and those from the selected polynomial model fit to the same sets of data.

Once the appropriate model was selected (Section 3.1), HRCs generated from the data sets collected during our experimental study were analysed in the same way for *A. loripes*, *A. abrotanoides*, *A. cf. microphthalma* and *A. elseyi*. The relevant oxyregulatory descriptive statistics ( $T_{\text{pos}}$ ,  $P_{\text{cmax}}$  and  $P_{\text{cmin}}$ ) were then extracted using Equation (1) for comparison. We note that since the selected colonies were independent and from different sites, we did not make inter-colony comparisons. Instead, we used (i) independent sample *t*-tests to compare intra-colony differences for each species (i.e., between the interior vs. exterior thicket samples), and (ii) completed a correlation analysis to compare whether differences between the ‘average’ regulation (i.e.,  $T_{\text{pos}}$ ) values measured in the interior/exterior coral fragments from the HRCs, corresponded with changes in DO ( $\text{mg O}_2 \text{ L}^{-1}$ ) measured from the loggers deployed at the same positions (as further described below).

## 2.4.2 | In situ $\text{O}_2$ logger data analysis

Environmental  $\text{O}_2$  levels ( $\text{DO}$ ,  $\text{mg O}_2 \text{ L}^{-1}$ ) were evaluated using independent sample *t*-tests to compare any differences between ambient  $\text{O}_2$  measured via the robust  $\text{O}_2$  probes positioned at the interior thickets and the exterior section of the individual colonies of *A. abrotanoides*, *A. cf. microphthalma*, and *A. elseyi*. Additionally, diel cycle information (i.e., sunrise/sunset times) and tidal times (hh:mm:ss) and tidal height (m) data were collected for Opal Reef over the experimental period (BOM, 2023; WillyWeather, 2023), and plotted against the environmental  $\text{O}_2$  and temperature ( $^{\circ}\text{C}$ ) data collected, to decipher whether the  $\text{O}_2$  profiles corresponded with tidal flushing, and/or diel cycle variance. Furthermore, cumulative histograms were prepared to show accumulative time spent (%) at each level of dissolved  $\text{O}_2$  measured within the individual colonies, to make supplementary intra-colony comparisons.

## 3 | RESULTS

### 3.1 | Model analysis and selection: *A. hyacinthus*, *A. intermedia* and *A. kenti*

The linear (1st degree) model was consistently the ‘worst’ fit according to the AIC and Residual Sum of Squares (RSS, i.e., the highest value) for every replicate ( $n=3$ ) of the three *Acropora* species: *A. hyacinthus*, *A. intermedia* and *A. kenti* (Figure 1b, and Table 2; example species *A. kenti* shown, see Figures S1 and S2 for *A. hyacinthus* and *A. intermedia*). However, and as expected, the 10th- or 12th-order polynomials generally returned the lowest AIC and RSS values (Table 2, Figures S1 and S2), suggesting ‘best’ fit, most likely from the higher number of degrees of freedom, and modelling inflexion points fitting directly through the data points (Figure 1g,h). Interestingly, during this model fit process, one replicate of *A. kenti* selected the Michaelis–Menten (MM) as the best fit function, with the lowest AIC for that group (Figure 1c; Rep 2, AIC  $-239.72$ ), which similar to (Hughes, Alexander, et al., 2022), was also chosen specifically as the best fit for one replicate. As per (Hughes, Alexander, et al., 2022), a MM fit chosen as the ‘best model’ suggests a continuous regulatory process within the organism.

Extracted  $T_{\text{pos}}$ ,  $P_{\text{cmax}}$  and  $P_{\text{cmin}}$  values from models with fewer degrees of freedom (2nd through to 8th order), for all *Acropora* species, were all within the same order of magnitude as per previously extracted values (Table 2). For example, mean  $T_{\text{pos}}$  for *A. kenti* extracted from the re-fit using the MM model ( $T_{\text{pos}}=0.77$ ) was half that of the original extracted parameter from the fit by Hughes, Alexander, et al. (2022) ( $T_{\text{pos}}=1.55$ ; Table 2, and Figure 2a), but not significantly lower ( $t_{(4)}=2.74$ ,  $p>.05$ ). In fact, there were no significant differences between any of the extracted parameters ( $T_{\text{pos}}$ ,  $P_{\text{cmax}}$ ,  $P_{\text{cmin}}$ ), between the original and MM re-fit models, for any of the three *Acropora* species (*t*-tests; Table S1). In general, the extracted values above the 10th-order polynomial fits were much higher and did not

**TABLE 2** Mean descriptive statistics and model fit data extracted from models of varying polynomial degrees with varying degrees of freedom (from 1st through to 12th order), fit to hypoxia response curve data sets ( $n=3$ ) of *Acropora kenti* (data from Hughes, Alexander, et al., 2022); including total positive regulation ( $T_{\text{pos}}$ , relative units), the  $p\text{O}_2$  value (% air saturation) at which maximum and minimum regulation ( $P_{\text{cmax}}$  and  $P_{\text{cmin}}$ ) occur, and model fit parameters including Akaike Information Criterion (AIC), and Residual Sum of Squares (RSS) for the model fits (where the lowest values signify the “best fit”).

Model fit	Free parameters	$T_{\text{pos}}$ (relative)	$P_{\text{cmax}}$ (%)	$P_{\text{cmin}}$ (%)	AIC	RSS
Linear	1	NA	NA	NA	-193.02	0.49
Michaelis-Menten	2	0.77	11	94	-281.58	0.17
Constrained Quartic	4	0.73	73	45	-261.13	0.19
Constrained Sextic	6	0.84	69	80	-283.79	0.15
Constrained Octic	8	0.92	34	75	-295.87	0.13
Constrained Decic	10	2.44	64	45	-295.89	0.12
Constrained Dodecic	12	79.42	33	30	-296.60	0.12
Hughes, Alexander, et al. (2022)	12	1.55	17	49	NA	NA

align with the previously reported numbers (Table 2), suggesting an overfit of the data with these selected models.

Additionally, we performed a correlation analysis of the independent variables extracted from HRCs ( $T_{\text{pos}}$ ,  $P_{\text{cmax}}$ ,  $P_{\text{cmin}}$ ), based on those retrieved from (Hughes, Alexander, et al., 2022) versus our MM model re-fit (Figure 2f–h). Of the three *Acropora* species, an especially strong correlation was evident between the parameters extracted for *A. kenti*. Specifically, for  $P_{\text{cmax}}$  ( $r_{(2)}=.90$ ,  $p=.29$ ) with a high coefficient of determination ( $R^2$ ) of .81, and no significant difference between the means of the two groups—as well as  $T_{\text{pos}}$ , with a strong positive correlation,  $r_{(2)}=.87$ ,  $p=.33$ , and an  $R^2$  of .76 (not shown). However, across all three species, there were no significant differences between the means of the two groups ( $p$ -value  $>.05$ ), and there was a moderate positive relationship between the  $T_{\text{pos}}$  values ( $r_{(7)}=.19$ ,  $p=.63$ ) and  $P_{\text{cmax}}$  ( $r_{(7)}=.49$ ,  $p=.18$ ), and a weak negative relationship between the values for  $P_{\text{cmin}}$  ( $r_{(7)}=.12$ ,  $p=.75$ ; Figure 2f–h). See also Figure 2g where *A. hyacinthus* Rep 2 and Rep 3 have been annotated on the correlation analysis scatterplots.

Since parameters extracted from the models with fewer degrees of freedom were not significantly different from the original data sets, and the biological rationale for the number of inflexion points required to fit HRCs remains unclear, we selected the most parsimonious model to minimise the degrees of freedom. The Michaelis-Menten function—a 2-parameter kinetics-type function more commonly seen applied to enzyme reactions (Roskoski, 2015; Wood, 2018)—best captured the shape and nature of the data, across all three *Acropora* data sets analysed, with a more conservative approach using fewer free parameters. Following this selection, the MM fit was then applied to all HRCs for *Acropora* data sets collected during our experimental study, and the relevant oxyregulatory descriptive statistics ( $T_{\text{pos}}$ ,  $P_{\text{cmax}}$ ,  $P_{\text{cmin}}$ ) were extracted and analysed.

### 3.2 | Experiment 1—Fragmentation effects: *A. Loripes*

The mean drawdown rate from 100% to 0%  $p\text{O}_2$  (% air sat) of coral fragments left to recover for 7 days (hereafter referred to as ‘clipped’)

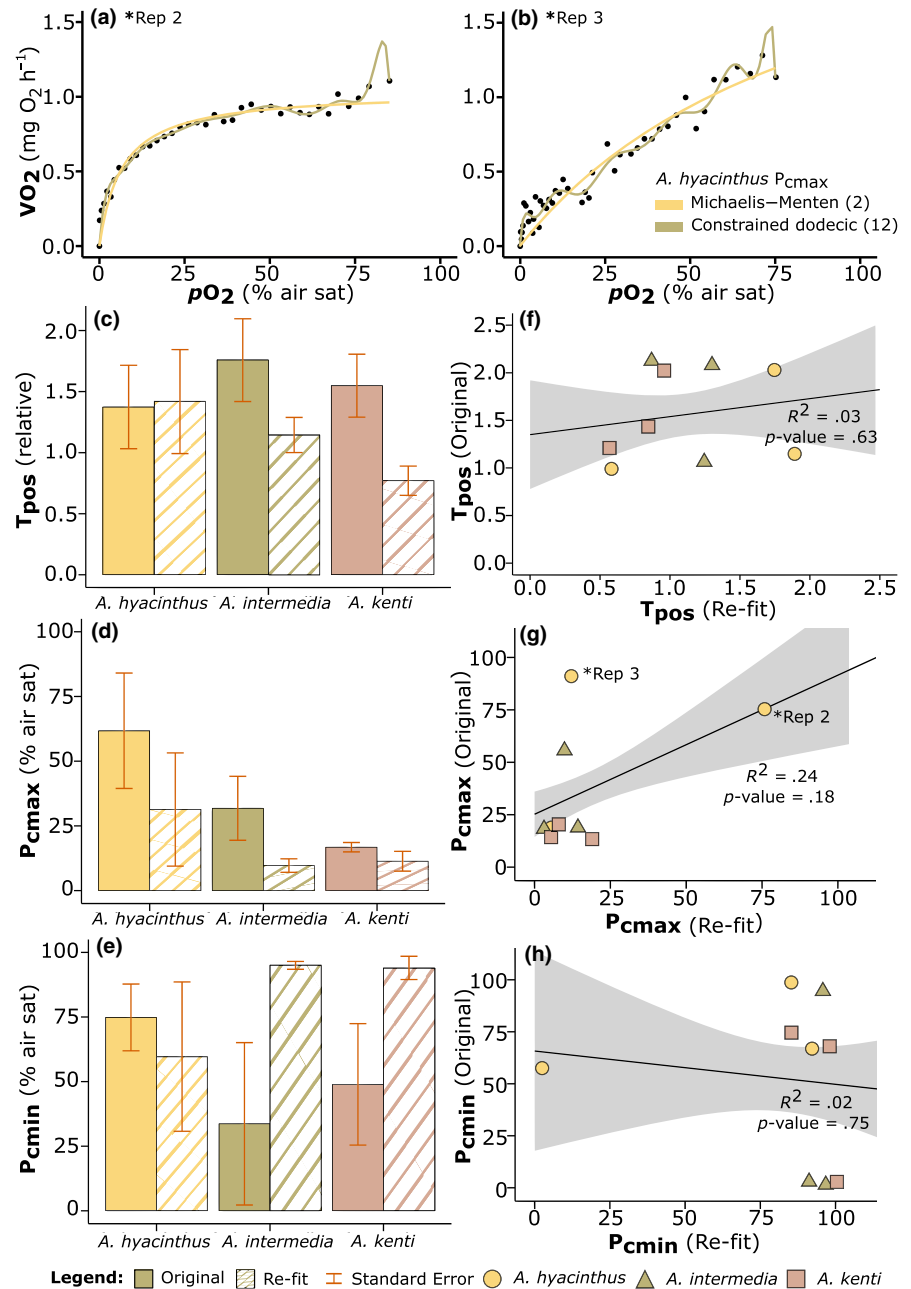
was 1.36 times faster than that for freshly fragmented corals, but not significantly lower ( $t_{(5)}=2.57$ ,  $p=.28$ ; Table S2A), at  $2.85\text{ h} \pm \text{SE } 0.47$ , compared to  $3.86\text{ h} \pm \text{SE } 0.70$ , respectively. Total positive regulation was also higher for the clipped fragment ( $T_{\text{pos}}=2.21 \pm \text{SE } 0.37$ ) compared to the fresh fragment ( $T_{\text{pos}}=1.71 \pm \text{SE } 0.27$ ; Figure 3a), but again no significant difference between the two groups ( $t_{(10)}=1.11$ ,  $p=.29$ ). In general, values for both  $P_{\text{cmax}}$  and  $P_{\text{cmin}}$ —that is, the  $p\text{O}_2$  level (% air sat) at which maximum/minimum regulation occurred—were lower in the clipped fragments, compared with the freshly fragmented corals. Specifically,  $P_{\text{cmax}}$  for both the clipped and freshly fragmented corals performed their maximum regulation effort at relatively low  $p\text{O}_2$ , below 14% air saturation, with no difference between treatments ( $t_{(10)}=0.95$ ,  $p=.37$ ; Figure 3b, Table S2A). Corals in both treatments exerted minimum regulation effort ( $P_{\text{cmin}}$ ) at similar  $p\text{O}_2$ ,  $89.17\% \pm \text{SE } 1.60$ , and  $92.17\% \pm \text{SE } 1.58$  (Figure 3c), for the clipped and fresh fragments, respectively. Collectively, these data confirmed that mean  $\text{O}_2$  drawdown rates and oxyregulatory capacity remained the same whether corals were freshly fragmented or were provided with 7 days recovery post fragmentation.

### 3.3 | $\text{O}_2$ logger data: *A. abrotanoides*, *A. cf. micropthalma*, and *A. elseyi*

For the three *Acropora* species at Opal Reef, seawater temperature and overall  $\text{O}_2$  profiles appeared to reflect diel cycles (e.g., time of day) more than tidal height (Figure 4). This resulted in all examined coral colonies spending 47% of time between 5.50 and 6.50  $\text{mg O}_2 \text{ L}^{-1}$  (Figure S3). Note that 100% air saturation here corresponds to  $7.67 \text{ mg L}^{-1}$ , calculated at 1013 mbar, 35 ppt salinity and the average recorded temperature  $29.12^\circ\text{C}$  (Figure 4). Dissolved  $\text{O}_2$  concentrations (DO) measured within the *A. abrotanoides* colony spanned 5.46–9.63  $\text{mg L}^{-1}$  (Figure 4a), in comparison with the *A. elseyi* colony, with measurements ranging 3.74–7.81  $\text{mg L}^{-1}$  within the interior thickets, and 4.71–13.80  $\text{mg L}^{-1}$  for the exterior branches (Figure 4c; Figure S3). At no time over the recorded period, did the DO drop below  $<2 \text{ mg L}^{-1}$  (i.e., a commonly used threshold for hypoxia); however, in the *A. elseyi* colony, 7% of time



**FIGURE 2** (a) and (b) *Acropora hyacinthus* hypoxia response curve (HRC) data set Rep 2 and Rep 3, fit with 2-parameter Michaelis–Menten (MM) function (yellow line), and 12th-order constrained dodecic model (green line). Reps 2 and 3 also annotated on (g)  $P_{cmax}$  scatterplot | (c–e) Extracted parameters:  $T_{pos}$  (relative units),  $P_{cmax}$  and  $P_{cmin}$  (% air saturation) from HRC data as analysed by Hughes, Alexander, et al. (2022) i.e., ‘Original’ (solid colour), and re-analysed here, that is, ‘Re-fit’ (striped colour) using the MM model, of *Acropora* species ( $n=3$ ): *A. hyacinthus*, *A. intermedia*, and *A. kenti*. Error bars are calculated standard error. | (f–h) correlation analyses of the same extracted data:  $T_{pos}$ ,  $P_{cmax}$ , and  $P_{cmin}$ , from original fits (y-axes), and from re-fit curves using MM model (x-axes). Linear  $R^2$  values calculated across averages (shown as the solid black line), and Pearson's Correlation Coefficients (not shown):  $T_{pos}=0.19$ ,  $P_{cmax}=0.49$ , and  $P_{cmin}=0.12$ , and the significance of the correlation coefficients (where  $p$ -value  $< .05$  is considered significant, shown). Shading indicates the 90% confidence interval.



was spent below  $5 \text{ mg O}_2 \text{ L}^{-1}$  in the interior thickets, compared to  $<1\%$  in the exterior (Figure S3). Indeed, the greatest difference in DO ( $\text{mg O}_2 \text{ L}^{-1}$ ) measured between the interior and exterior of the *Acropora* colonies was observed for *A. elseyi* ( $t_{(11620)} = -50.55$ ,  $p < .001$ ; Table S3) consistently over most tidal and diel changes (Figure 4c). Whilst DO of the *A. cf. microphthalma* colony was also significantly higher for the exterior than interior ( $t_{(8400)} = -10.92$ ,  $p < .00$ ), this trend was generally only seen during the middle of the day, which aligned with fragment sampling time (Figure 4b). Overall, DO differences between inner and outer colony locations were small, however, it is evident that DO measured at the interior section were on average  $\sim 10\%$  lower than the exterior, suggesting intra-colony-specific spatial variation in the  $\text{O}_2$  levels of the seawater surrounding coral branches.

### 3.4 | Experiment 2—Interior versus exterior colony HRC variance: *A. abrotanoides*, *A. cf. microphthalma* and *A. elseyi*

For all three *Acropora* species, the mean ( $n=6$ ) total positive regulation ( $T_{pos}$ ), and  $p\text{O}_2$  (% air sat) at which the minimum regulation effort occurred ( $P_{cmin}$ ), was greater for fragments sampled from the interior than exterior of the coral thickets (Figure 5b,d). Specifically, mean  $P_{cmin}$  for *A. elseyi* occurred at a significantly higher  $p\text{O}_2$  for the interior ( $96.17\% \pm \text{SE } 0.40$ ) than the exterior fragments ( $94.50\% \pm \text{SE } 0.62$ , Figure 5d,  $t_{(10)} = 2.26$ ,  $p = .05$ , Table S2B). Except for *A. abrotanoides*, where  $P_{cmax}$  was the same on average ( $P_{cmax} = 4.83\%$ ) across interior and exterior samples (Figure 5c), the level at which maximum regulation effort occurred was at a higher  $p\text{O}_2$  (% air sat) in

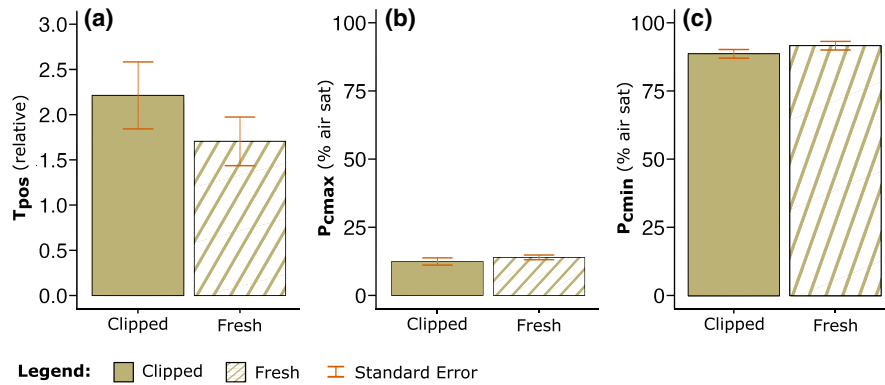


**FIGURE 3** Comparison of the extracted parameters: (a)  $T_{pos}$  (relative units), (b)  $P_{cmax}$ , and (c)  $P_{cmin}$  (% air saturation) from hypoxia response curve data of replicates ( $n=6$ ) of *Acropora loripes*. Plots compare extracted parameters from fragments clipped to the reef substrate for 7 days using the CoralClip® (solid colour), and extractions from samples freshly fragged (striped colour), fit with the selected Michaelis-Menten model. Error bars are calculated standard error.

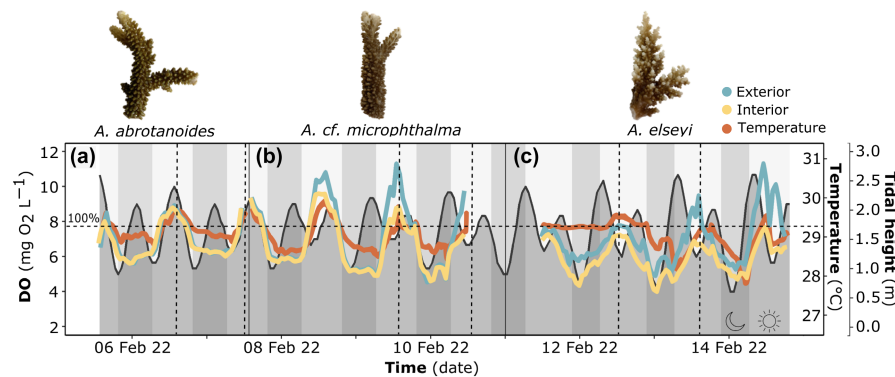


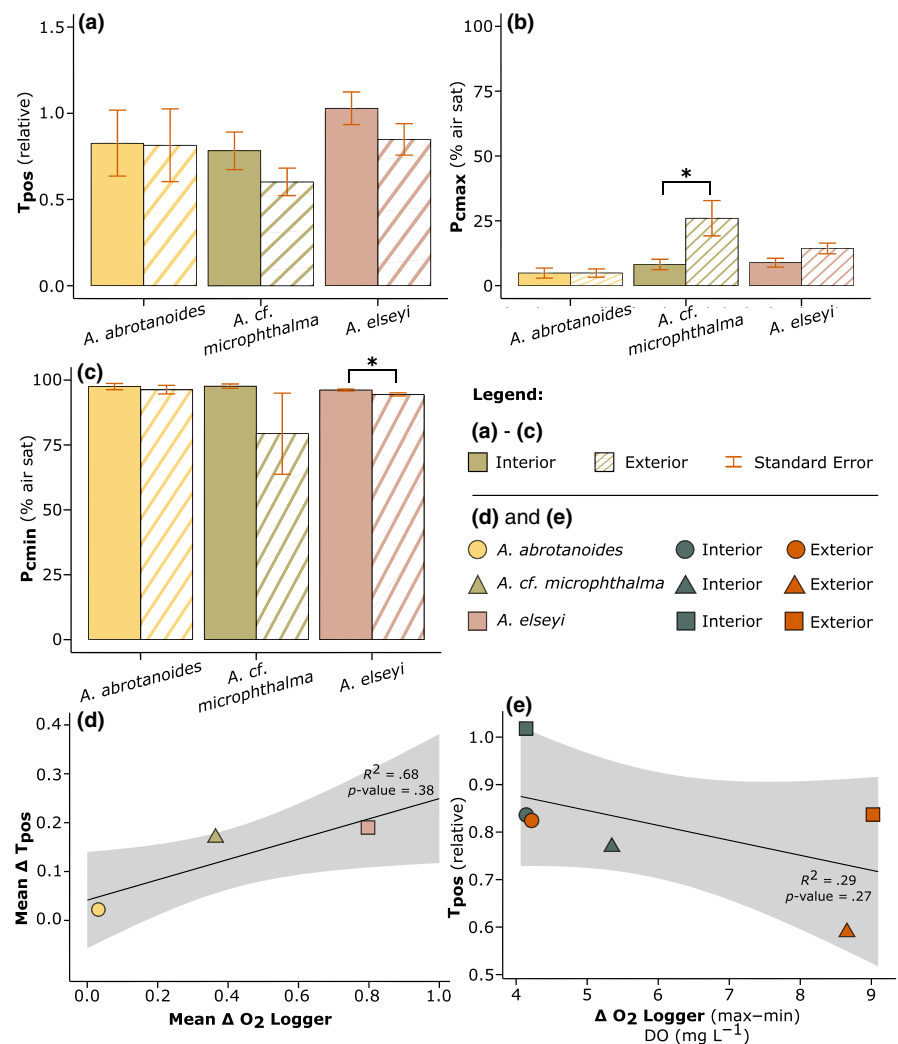
**FIGURE 4** Dissolved oxygen (DO) content ( $\text{mg O}_2 \text{ L}^{-1}$ ) displayed on the left y-axis was measured at the interior (yellow) and exterior (blue) sections of the three branching *Acropora* colonies; panels (a) *A. abrotanoides*, (b) *A. cf. microphthalma*, and (c) *A. elseyi*, respectively. Ambient water temperature (orange,  $^{\circ}\text{C}$ ) on the inside right y-axis, was also measured by the loggers deployed in the sample colonies, and is coupled with tidal height (dark shaded area with black outline, m) on the outside right y-axis. Daily light cycles are represented by vertical shading and signified by the sun and moon symbols, over time on the x-axis (date). Note that vertical dashed lines indicate fragment sampling times for each *Acropora* colony, carried out over the experimental period (as summarised in Table 1), whilst the horizontal dashed line indicates 100% air sat (i.e., at  $\sim 7.67 \text{ mg O}_2 \text{ L}^{-1}$ ).

the exterior than interior fragments, and significantly higher in *A. cf. microphthalma* (at  $26\% \pm \text{SE } 6.80$ ), compared to  $8.17\% \pm \text{SE } 2.01$  ( $t_{(10)} = 2.51$ ,  $p = .03$ , Figure 5c). Despite the lack of statistical significance between the interior versus exterior  $T_{pos}$  values (Figure 5b), differences between the intra-colony average regulation ( $T_{pos}$ ), were highly consistent with changes in dissolved  $\text{O}_2$  (DO,  $\text{mg O}_2 \text{ L}^{-1}$ ) measured between the inner and outer colony locations, for all species (Figures 4 and 5). Between the average  $\Delta \text{DO}$  logger data (DO,  $\text{mg O}_2 \text{ L}^{-1}$ ; Figure 4a-c) and the average  $\Delta T_{pos}$  data (relative units; Figure 5b), there was a positive correlation, albeit non-significant ( $r_{(1)} = .83$ ,  $p = .38$ ) – with a high coefficient of determination ( $R^2 = .68$ ; Figure 5a; Table S2B).

A weak negative correlation ( $R = .54$ ,  $R^2 = .29$ ) was also evident between the dynamic range of DO ( $\text{mg O}_2 \text{ L}^{-1}$ ) measured by the  $\text{O}_2$  loggers (max-min), and  $T_{pos}$ , on average (Figure 5e), showing that less DO variation results in higher  $T_{pos}$ . For example, the

maximum range of DO measured in the interior section of the *A. elseyi* colony ( $4.06 \text{ mg O}_2 \text{ L}^{-1}$ ) – which is the smallest range in DO overall – corresponds to the highest  $T_{pos}$  on average ( $1.03 \pm \text{SE } 0.09$ ) (Figure 5a,e). Additionally, in both *A. abrotanoides* and *A. elseyi*,  $\text{O}_2$  drawdown rate (% air sat) was slightly faster in the fragments taken from the interior section of the colonies, compared with the exterior thickets, by 103% and 105%, respectively (see Table S4 for mean  $\text{O}_2$  drawdown rates (h)). However, for *A. cf. microphthalma*, the  $\text{O}_2$  drawdown rate was 131% faster in the exterior fragments ( $6.94 \text{ h} \pm \text{SE } 0.64$ ), which was significantly more rapid in comparison with fragments sampled from the interior ( $9.07 \text{ h} \pm \text{SE } 0.87$ ,  $t_{(5)} = 2.57$ ,  $p = .01$ ; Table S4). High variance across the sampling – albeit not statistically significant across most comparisons of extracted HRC parameters – indicates that even within intra-colony sampling (i.e., interior/exterior), fragments are characterised by inherently high variation in respiration.

**FIGURE 5** (a–c) Comparison of the extracted parameters:  $T_{pos}$  (relative units),  $P_{cmax}$  and  $P_{cmin}$  (% air saturation) from HRC data of replicates ( $n=6$ ) of *Acropora* species: *A. abrotanoides*, *A. cf. microphthalma*, and *A. eleyi*. Plots compare extracted parameters from fragments taken from the interior section of the colony (solid colour), and fragments from the exterior thickets (striped colour), fit with the selected MM model. Error bars are calculated standard error. Note that significance levels (where  $p$ -values  $< .05$  considered significant) are identified by a bold \* above relevant data. (d) Correlation analysis between mean interior and exterior delta ( $\Delta$ )  $O_2$  logger data (DO,  $mg\ L^{-1}$ ) and  $\Delta T_{pos}$  data (relative units), between species. Linear  $R^2$  was calculated across means (shown as the solid black line), as well as Pearson's Correlation Coefficient = 0.83, and the significance of the correlation coefficient (also shown). (e) Additional correlation analysis between  $\Delta O_2$  logger range (max-min), and  $\Delta T_{pos}$  data, between species, with Pearson's Correlation Coefficient = 0.54, and linear  $R^2$  and significance of correlation coefficient (shown). Shading is 90% confidence interval.



## 4 | DISCUSSION

Coral reefs worldwide are under significant threat from the relatively unstudied process of ocean deoxygenation (Hughes et al., 2020; Pezner et al., 2023; Pontes et al., 2023; Sampaio et al., 2021), in comparison to the well-known stressors of ocean warming and acidification. Thresholds and performance dynamics with which corals respond to losses of  $O_2$  remain limited, with only few experimental assessments to date (Alderdice et al., 2021; Alva García et al., 2022; Hughes et al., 2020; Johnson, Scott, et al., 2021; Nelson & Altieri, 2019) since real-time deoxygenation events are difficult to capture in the field. Such limited knowledge therefore limits current capacity to predict how corals—and in turn coral reefs—will respond to future anthropogenically-driven declines in reef  $O_2$  levels. Here, we examined dynamics of  $O_2$  performance for species of *Acropora* common on the GBR, where previous studies have identified species from this genus to exhibit highly variable responses to both time-dependent (Alderdice et al., 2021; Johnson, Scott, et al., 2021) and dose-dependent (Haas et al., 2014) analyses, including HRCs (Hughes, Alexander, et al., 2022). We used initial methodological steps to (a) demonstrate that a simpler model can be used to analyse coral HRCs than previously examined, and (b) establish

that immediate fragmenting does not induce added stress during  $O_2$  drawdown, when compared to fragmenting with a seven-day recovery-period. Subsequent measurements of both DO and HRCs for interior versus exterior colony thickets—where the two factors correspond—also exhibited within-colony variability between species.

### 4.1 | Modelling and experimental considerations in describing $O_2$ physiology

HRC models have been used to examine how various aquatic organisms including fish (Cobbs & Alexander, 2018; Ultsch & Regan, 2019; Zhang & Farrell, 2022) and corals (Dodds et al., 2007; Hughes, Alexander, et al., 2022) respond to declining  $O_2$  levels. Experimental HRCs have been analysed with a multitude of oxyregulatory descriptive statistics to parameterise organism  $O_2$  sensitivity. However, models that fit specific data sets better than others may not necessarily reflect a more accurate model, but rather that the selected model has greater 'fit propensity', that is, may fit a larger range of data inadequately, as opposed to a more accurate fit across a smaller range (Falk & Muthukrishna, 2023). Our model analysis demonstrates

the challenges of collecting repeatable data without noise, which becomes more apparent when selecting towards a higher polynomial degree (e.g., constrained dodecic, 12th order, Figure 1h). Specifically, greater variance in HRC data results in lower correlation between models (e.g., between the 2nd-order MM, and 12th order polynomial; see Figure 2b *A. hyacinthus* Rep 3). In contrast, more convergence between the two models, with a higher correlation, is evident when HRC data are less variable (e.g., see Figure 2a *A. hyacinthus* Rep 2). Scattered data for any given HRC demonstrate the high variability in organism respiration, and for corals specifically, the unknown physiological mechanisms occurring between 100% and 0%  $pO_2$  that an organism may employ when DO reaches a certain level. Therefore, we argue that relying on a more conservative model with fewer degrees of freedom (e.g., 2-parameter MM; Figure 1c) appears more lenient in terms of the challenges of analysing physiological data, ensuring more consistency across biological replicates whilst avoiding overfitting data with higher order models, as evident in Figure 1. However, as our understanding of the physiological mechanisms that the coral holobiont employs during increasingly low levels of  $O_2$  improves, higher polynomial models may become more appropriate, and can thus be selected based on the known biological mechanisms at play.

## 4.2 | $O_2$ and HRC dynamics of *Acropora* species

The  $O_2$  dynamics in coral colonies is strongly affected by the flow of seawater around and within the colonies, which is in turn affected by coral colony size and morphology, including distance between branches and branch diameter (Hossain & Staples, 2020; Hughes et al., 2020). Interactions between flowing seawater and coral structure lead to formation of hydromechanical (Shashar et al., 1996), diffusive (Kühl et al., 1995) and thermal (Jimenez et al., 2008) boundary layers that affect mass and heat transfer between the coral and surrounding seawater. Flow dynamics and boundary layers are not only species-specific, but dependent on colony-specific morphological structures (Hossain & Staples, 2020; Jimenez et al., 2011) and coral behavioural features such as ciliary movement induced vortices and local advective flows (Pacherres et al., 2022) and transport between polyps (Bouderlique et al., 2022). We note that the  $O_2$  budget of tropical corals is partitioned between the coral animal host, its microalgal symbionts, and microbiomes associated within the coral tissue, gastric cavity and coral skeleton (Hughes, Raina, et al., 2022), but the relative importance of these different compartments for observed responses of the coral holobiont to declining  $O_2$  levels remain unknown. The  $O_2$  supply of corals can be further modified by fish ventilation, especially under low ambient  $O_2$  conditions where hyperventilation in gill pumping occurs (Zhang & Farrell, 2022), or by additional respiration from commensal organisms within corals, such as the guard crab *Trapezia* (McKeon & Moore, 2014).

Here, we recorded subtle differences in the ambient DO ( $mg O_2 L^{-1}$ ) levels, measured at the interior and exterior sections of the

three selected *Acropora* colonies for experimental sampling: *A. abrotanoides*, *A. cf. microphthalma* and *A. eleyi*. Whilst we were unable to quantitatively resolve differences in factors that may have impacted flow penetration into the colonies examined here, it is intriguing that the greatest difference in intra-colony recorded DO occurred in *A. eleyi* with an apparent more tightly formed thicket colony structure (Figure 4c and Table 1, Line 4). In contrast, the smallest difference was recorded between interior and exterior branches in *A. abrotanoides*—that exhibits a relatively more spaced-out colony geometry (Figure 4a and Table 1, Line 2). This is further amplified by the weak but positive correlation ( $R^2 = .68$ , Pearson's Correlation Coefficient = 0.83, see Figure 5d), albeit statistically insignificant ( $p$ -value > .05), between the  $\Delta$  interior versus exterior  $T_{pos}$  values measured in all three *Acropora* species, and the  $\Delta$  interior/exterior DO content ( $mg O_2 L^{-1}$ ), indicating that differences between the intra-colony average regulation, were highly consistent with changes in DO.

We show a range of highly variable hypoxic thresholds for oxygen regulation, with total positive regulation capacity varying from 0.60 to 1.03 ( $T_{pos}$ , relative) across species, which aligns with the high variation in hypoxic tolerance seen previously in *Acropora* species (Deleja et al., 2022; Hughes, Alexander, et al., 2022; Pontes et al., 2023). For example, *A. cervicornis* had the second lowest  $pO_2$  crit (critical oxygen partial pressure) of  $2.22 mg O_2 L^{-1}$  (i.e.,  $7 \pm 1 kPa$ ; Pontes et al., 2023), in a study out of six species of Caribbean scleractinian corals (Pontes et al., 2023). A lower  $pO_2$  crit ( $P_{crit}$ ) is suggested to be an advantageous characteristic for surviving low  $O_2$  periods (Nilsson & Östlund-Nilsson, 2005; Pontes et al., 2023) – similarly to the low  $P_{cmax}$  values ascertained here. On average, *A. abrotanoides* exerted maximum regulation effort at lower  $pO_2$  (% air sat) values (i.e., under low ambient DO) in comparison to all other corals ( $4.83\% \pm SE 1.24$ ), for both interior and exterior fragments (Figure 5b; Table S2B), with the highest  $P_{cmax}$  value recorded in this study at 26% air sat (*A. cf. microphthalma* exterior; Figure 5c). These  $P_{cmax}$  values are lower than the lowest observed on average across all coral taxa as analysed by (Hughes, Alexander, et al., 2022) at around 30% air sat—and within a similar range to those noted for coral reef fishes ~10–25% air sat (measured as  $P_{crit}$ ) (Nilsson & Östlund-Nilsson, 2005). However, we acknowledge that the more conservative approach to modelling adopted here (with fewer degrees of freedom) may account for the lower values seen across descriptive statistics. Nonetheless, *Acropora* therefore appears to be a highly dynamic species, across both hypoxic landscapes (Alderdice et al., 2021; Deleja et al., 2022; Haas et al., 2014; Hughes, Alexander, et al., 2022; Pontes et al., 2023), and additionally in thermal tolerance to heat stress (Alderdice et al., 2022; Hoogenboom et al., 2017; Nielsen et al., 2022).

Whilst the hypoxia threshold of  $<2 mg O_2 L^{-1}$  (or ~25% air sat) is widely cited (Altieri et al., 2021; Hughes et al., 2020; Hughes, Alexander, et al., 2022; Rabalais et al., 2001; Vaquer-Sunyer & Duarte, 2008)—and although the specific threshold for *Acropora* species is unclear—a general universal threshold may not prove useful simply due to the high variability in sampling (e.g.,  $T_{pos}$  as seen

here), including across other experimental studies. For example, a recent study by Johnson, Scott, et al. (2021) recorded lethal thresholds for the Caribbean coral *Acropora cervicornis* after just 1 day of exposure at  $1 \text{ mg O}_2 \text{ L}^{-1}$ , in comparison with the highly variable hypoxia thresholds for upregulation recorded here i.e.,  $P_{\text{cmax}}$  ranging from 4.83% to 26% air sat (or  $\sim 0.38$  to  $2.03 \text{ mg O}_2 \text{ L}^{-1}$ ; Figure 5). No periods of potential hypoxia were recorded during logger deployment across any of the *Acropora* colonies, where DO did not drop below  $3.5 \text{ mg L}^{-1}$  (Figure 4a–c). However, it is important to note here that  $\text{O}_2$  concentrations within the diffusive boundary layer are likely considerably lower at night even within the colony, in comparison with  $\text{O}_2$  levels measured in the water column (Kühl et al., 1995; Shashar et al., 1993, 1996).

Notably, what we have shown is the DO span these *Acropora* species can tolerate, relative to their average regulation ( $T_{\text{pos}}$ ) characteristics—where different range exposures over the interior and exterior colony, result in different thresholds of  $T_{\text{pos}}$ . Although weak, there is a negative correlation between the range ( $\Delta$  max–min interior and exterior) of DO ( $\text{mg O}_2 \text{ L}^{-1}$ ), and the mean  $T_{\text{pos}}$ , where lower variation in DO corresponds to a higher  $T_{\text{pos}}$  (Figure 5e). Even with the lowest range in DO overall, *A. abrotanoides* still has a higher  $T_{\text{pos}}$  on average ( $0.82 \pm \text{SE } 0.20$ ) than *A. cf. microphthalma* ( $0.69 \pm \text{SE } 0.09$ ; Figure 5a) which has a greater dynamic range in DO, across both the interior and exterior colony (Figures 4 and 5e). Additionally, *A. eleyi* had the highest  $T_{\text{pos}}$  on average, measured at the interior fragments specifically, but also across all three *Acropora* species ( $1.03 \pm \text{SE } 0.09$ ), suggesting the greatest ‘average’ regulation across the colonies sampled.

The dynamic range of DO, and extremely high variability in regulation across intra-colony sampling seen here, with high standard error between replicates ( $n=6$ ) for all species, would suggest that even within location sampling (i.e., between the interior and exterior fragments), there is high variation in the respiration rates of corals, which affects within-colony oxyregulatory capacity. Therefore, among other sampling considerations—e.g., fragment size and sampling time, for heat stress assays (Nielsen et al., 2022)—the outcomes from our methodological findings confirm that, (i) having multiple replicates is essential for producing repeatable data, (ii) although coral respiration rates are highly variable, fragment collection does not appear to induce additional stress to alter  $\text{O}_2$  physiological parameterisation, and (iii) albeit ‘non-significant’ (likely due to the large standard error across sampling) there does seem to be intra-colony  $\text{O}_2$  spatial variance, which would be amplified further, without specific location sample acquisition. Additionally, conservative parameterisation of HRC model fitting can yield comparative oxyregulatory statistics to models with a higher number of polynomial degrees, without over-fitting inflexion points of unknown biological origin. Our data add insight into coral HRC analysis, expanding on the inventories of hypoxic thresholds for upregulation and oxyregulatory capacity for the key coral reef-building species *Acropora*—including intra-colony spatial  $\text{O}_2$  variation—as well as expanding on considerations

for future fragment sampling collection. Ocean deoxygenation is an emergent threat to coral reefs worldwide, and therefore must be a consideration in future studies in conjunction with the effects of other well-studied stressors under climate change (e.g., ocean warming and acidification), including oxyregulatory capacity of corals under warming oceans, since increased temperatures increases biological  $\text{O}_2$  demand (Alderdice et al., 2022; Keeling et al., 2010; Pezner et al., 2023).

## AUTHOR CONTRIBUTIONS

**Nicole J. Dilernia:** Conceptualization (lead); data curation (lead); formal analysis (lead); investigation (lead); methodology (lead); resources (lead); software (lead); validation (lead); visualization (lead); writing – original draft (lead); writing – review and editing (equal). **Stephen Woodcock:** Methodology (supporting); software (equal); writing – review and editing (supporting). **Emma F. Camp:** Conceptualization (supporting); methodology (supporting); project administration (equal); supervision (equal); writing – review and editing (equal). **David J. Hughes:** Conceptualization (supporting); methodology (supporting); supervision (equal); writing – review and editing (supporting). **Michael Kühl:** Resources (supporting); supervision (equal); writing – review and editing (supporting). **David J. Suggett:** Conceptualization (supporting); investigation (supporting); methodology (supporting); project administration (lead); supervision (equal); validation (supporting); writing – review and editing (supporting).

## ACKNOWLEDGEMENTS

We wish to express thanks to two anonymous Reviewers, whose comments greatly improved our manuscript. The authors would like to express thanks and acknowledge the staff and owners of Wavelength Reef Cruises for their assistance in providing reef access. As well as the Great Barrier Reef Marine Park Authority for their continued support and issuance of Permit No. G20/43740.1. N.J.D. would also like to specifically acknowledge Future Reefs Team members Lorna Howlett, Christine Roper, Paige Strudwick and Gemma Gillette, as well as Natasha Bartels and Amanda Grima, for their assistance during field work and sample collection in February 2022. Open access publishing facilitated by University of Technology Sydney, as part of the Wiley - University of Technology Sydney agreement via the Council of Australian University Librarians.

## FUNDING INFORMATION

This research is supported by an Australian Government Research Training Program Scholarship (N.J.D.) and an Australian Research Council Discovery Project (DP230100210) (awarded to: D.J.S., E.F.C., and M.K.). M.K. also acknowledges additional support from the Gordon and Betty Moore Foundation (grant no. GBMF9206; <https://doi.org/10.37807/GBMF9206>).

## CONFLICT OF INTEREST STATEMENT

No competing interests declared.



## DATA AVAILABILITY STATEMENT

The data and code that support the findings of this study are openly available in Dryad (<https://doi.org/10.5061/dryad.gtht76ht3>).

## ORCID

Nicole J. Dilernia  <https://orcid.org/0000-0002-0872-7402>

Stephen Woodcock  <https://orcid.org/0000-0003-4903-3164>

Emma F. Camp  <https://orcid.org/0000-0003-1962-1336>

David J. Hughes  <https://orcid.org/0000-0003-3778-7460>

Michael Kühl  <https://orcid.org/0000-0002-1792-4790>

David J. Suggett  <https://orcid.org/0000-0001-5326-2520>

## REFERENCES

- Aichelman, H. E., Zimmerman, R. C., & Barshis, D. J. (2019). Adaptive signatures in thermal performance of the temperate coral *Astrangia poculata*. *Journal of Experimental Biology*, 222, jeb189225. <https://doi.org/10.1242/JEB.189225>
- Alderdice, R., Perna, G., Cárdenas, A., Hume, B. C. C., Wolf, M., Kühl, M., Pernice, M., Suggett, D. J., & Voolstra, C. R. (2022). Deoxygenation lowers the thermal threshold of coral bleaching. *Scientific Reports*, 12, 1–14. <https://doi.org/10.1038/s41598-022-22604-3>
- Alderdice, R., Suggett, D., Cardenas, A., Hughes, D., Kühl, M., Pernice, M., & Voolstra, C. (2021). Divergent expression of hypoxia response systems under deoxygenation in reef-forming corals aligns with bleaching susceptibility. *Global Change Biology*, 27, 1–15. <https://doi.org/10.1111/gcb.15436>
- Allaire, J., Xie, Y., McPherson, J., Luraschi, J., Ushey, K., Atkins, A., Wickham, H., Cheng, J., Chang, W., & Iannone, R. (2023). *rmarkdown: Dynamic Documents for R* package version 2.25.3. <https://github.com/rstudio/rmarkdown>
- Altieri, A. H., Harrison, S. B., Seemann, J., Collin, R., Diaz, R. J., & Knowlton, N. (2017). Tropical dead zones and mass mortalities on coral reefs. *Proceedings of the National Academy of Sciences of the United States of America*, 114, 3660–3665. <https://doi.org/10.1073/pnas.1621517114>
- Altieri, A. H., Johnson, M. D., Swaminathan, S. D., Nelson, H. R., & Gedan, K. B. (2021). Resilience of tropical ecosystems to ocean deoxygenation. *Trends in Ecology & Evolution*, 36(3), 227–238.
- Alva García, J. V., Klein, S. G., Alamoudi, T., Arossa, S., Parry, A. J., Steckbauer, A., & Duarte, C. M. (2022). Thresholds of hypoxia of two Red Sea coral species (*Porites* sp. and *Galaxea fascicularis*).
- BOM. (2023). *Climate data online – Daily rainfall*. Bureau of Meteorology. Commonwealth of Australia. <http://www.bom.gov.au/climate/data/index.shtml>
- Bouderlique, T., Petersen, J., Faure, L., Abed-Navandi, D., Bouchnita, A., Mueller, B., Nazarov, M., Englmaier, L., Tesarova, M., Frade, P. R., Zikmund, T., Koehne, T., Kaiser, J., Fried, K., Wild, C., Pantos, O., Hellander, A., Bythell, J., & Adameyko, I. (2022). Surface flow for colonial integration in reef-building corals. *Current Biology*, 32, 2596–2609.e7. <https://doi.org/10.1016/j.cub.2022.04.054>
- Breitburg, D., Levin, L. A., Oschlies, A., Grégoire, M., Chavez, F. P., Conley, D. J., Garçon, V., Gilbert, D., Gutiérrez, D., Isensee, K., Jacinto, G. S., Limburg, K. E., Montes, I., Naqvi, S. W. A., Pitcher, G. C., Rabalais, N. N., Roman, M. R., Rose, K. A., Seibel, B. A., ... Zhang, J. (2018). Declining oxygen in the global ocean and coastal waters. *Science*, 359, eaam7240. <https://doi.org/10.1126/science.aam7240>
- Bridge, T. C. L., Cowman, P. F., Quattrini, A. M., Bonito, V. E., Sinniger, F., Harii, S., Head, C. E. I., Hung, J. Y., Halafihi, T., Rongo, T., & Baird, A. H. (2023). A tenuous relationship: Traditional taxonomy obscures systematics and biogeography of the '*Acropora tenuis*' (Scleractinia: Acroporidae) species complex. *Zoological Journal of the Linnean Society*, zlad062. <https://doi.org/10.1093/zoolinnean/zlad062>
- Carey, N., Galkin, A., Henriksson, P., Richards, J. G., & Sigwart, J. D. (2013). Variation in oxygen consumption among 'living fossils' (Mollusca: Polyplacophora). *Journal of the Marine Biological Association of the United Kingdom*, 93, 197–207. <https://doi.org/10.1017/S0025315412000653>
- Cobbs, G. A., & Alexander, J. E. (2018). Assessment of oxygen consumption in response to progressive hypoxia. *PLoS One*, 13, e0208836. <https://doi.org/10.1371/journal.pone.0208836>
- Deleja, M., Paula, J. R., Repolho, T., Franzitta, M., Baptista, M., Lopes, V., Simão, S., Fonseca, V. F., Duarte, B., & Rosa, R. (2022). Effects of hypoxia on coral photobiology and oxidative stress. *Biology*, 11, 1068. <https://doi.org/10.3390/biology11071068>
- Diaz, R., & Rosenberg, R. (1995). Marine benthic hypoxia: A review of its ecological effects and the behavioural response of benthic macrofauna. *Oceanography and Marine Biology: An Annual Review*, 33, 245–303.
- Dilernia, N. J., Camp, E. F., Bartels, N., & Suggett, D. J. (2023). Contrasting the thermal performance of cultured coral endosymbiont photo-physiology. *Journal of Experimental Marine Biology and Ecology*, 561, 151865. <https://doi.org/10.1016/J.JEMBE.2022.151865>
- Dodds, L. A., Roberts, J. M., Taylor, A. C., & Marubini, F. (2007). Metabolic tolerance of the cold-water coral *Lophelia pertusa* (Scleractinia) to temperature and dissolved oxygen change. *Journal of Experimental Marine Biology and Ecology*, 349, 205–214. <https://doi.org/10.1016/j.jembe.2007.05.013>
- Falk, C. F., & Muthukrishna, M. (2023). Parsimony in model selection: Tools for assessing fit propensity. *Psychological Methods*, 28, 123–136. <https://doi.org/10.1037/met0000422.supp>
- Fifer, J. E., Bui, V., Berg, J. T., Kriefall, N., Klepac, C., Bentlage, B., & Davies, S. W. (2022). Microbiome structuring within a coral colony and along a sedimentation gradient. *Frontiers in Marine Science*, 8, 805202.
- Fox, J., & Weisberg, S. (2019). *An R companion to applied regression* (3rd ed.). Sage Publications.
- Giomì, F., Barausse, A., Duarte, C. M., Booth, J., Agustí, S., Saderne, V., Anton, A., Daffonchio, D., & Fusi, M. (2019). Oxygen supersaturation protects coastal marine fauna from ocean warming. *Science Advances*, 5, eaax1814. <https://doi.org/10.1126/sciadv.aax1814>
- Haas, A. F., Smith, J. E., Thompson, M., & Deheyn, D. D. (2014). Effects of reduced dissolved oxygen concentrations on physiology and fluorescence of hermatypic corals and benthic algae. *PeerJ*, 2, e235. <https://doi.org/10.7717/peerj.235>
- Hoogenboom, M. O., Frank, G. E., Chase, T. J., Jurriaans, S., Álvarez-Noriega, M., Peterson, K., Critchell, K., Berry, K. L. E., Nicolet, K. J., Ramsby, B., & Paley, A. S. (2017). Environmental drivers of variation in bleaching severity of *Acropora* species during an extreme thermal anomaly. *Frontiers in Marine Science*, 4, 376.
- Hossain, M. M., & Staples, A. E. (2020). Effects of coral colony morphology on turbulent flow dynamics. *PLoS One*, 15, e0225676. <https://doi.org/10.1371/journal.pone.0225676>
- Hughes, D. J., Alderdice, R., Cooney, C., Kühl, M., Pernice, M., Voolstra, C. R., & Suggett, D. J. (2020). Coral reef survival under accelerating ocean deoxygenation. *Nature Climate Change*, 10, 296–307. <https://doi.org/10.1038/s41558-020-0737-9>
- Hughes, D. J., Alexander, J., Cobbs, G., Kühl, M., Cooney, C., Pernice, M., Varkey, D., Voolstra, C. R., & Suggett, D. J. (2022). Widespread oxyregulation in tropical corals under hypoxia. *Marine Pollution Bulletin*, 179, 113722. <https://doi.org/10.1016/J.MARPOLBUL.2022.113722>
- Hughes, D. J., Raina, J.-B., Nielsen, D. A., Suggett, D. J., & Kühl, M. (2022). Disentangling compartment functions in sessile marine

- invertebrates. *Trends in Ecology & Evolution*, 37, 740–748. <https://doi.org/10.1016/j.tree.2022.04.008>
- Jimenez, I., Kühl, M., & Larkum, A. (2008). Heat budget and thermal microenvironment of shallow-water corals: Do massive corals get warmer than branching corals? *Limnology and Oceanography*, 53, 1548–1561. <https://doi.org/10.4319/lo.2008.53.4.1548>
- Jimenez, I. M., Kühl, M., Larkum, A. W. D., & Ralph, P. J. (2011). Effects of flow and colony morphology on the thermal boundary layer of corals. *Journal of the Royal Society Interface*, 8, 1785–1795. <https://doi.org/10.1098/rsif.2011.0144>
- Johnson, M. D., Scott, J. J., Leray, M., Lucey, N., Bravo, L. M. R., Wied, W. L., & Altieri, A. H. (2021). Rapid ecosystem-scale consequences of acute deoxygenation on a Caribbean coral reef. *Nature Communications*, 12, 4522. <https://doi.org/10.1038/s41467-021-24777-3>
- Johnson, M. D., Swaminathan, S. D., Nixon, E. N., Paul, V. J., & Altieri, A. H. (2021). Differential susceptibility of reef-building corals to deoxygenation reveals remarkable hypoxia tolerance. *Scientific Reports*, 11, 1–12. <https://doi.org/10.1038/s41598-021-01078-9>
- Kassambara, A. (2023a). *ggpubr: "ggplot2" Based publication ready plots*. <https://CRAN.R-project.org/package=ggpubr>
- Kassambara, A. (2023b). *rstatix: Pipe-Friendly Framework for Basic Statistical Tests. R package version 0.7.2*. <https://rpkgs.datanovia.com/rstatix/>
- Keeling, R. F., Körtzinger, A., & Gruber, N. (2010). Ocean deoxygenation in a warming world. *Annual Review of Marine Science*, 2, 199–229. <https://doi.org/10.1146/annurev.marine.010908.163855>
- Killen, S. S., Christensen, E. A. F., Cortese, D., Závorka, L., Norin, T., Cotgrove, L., Crespel, A., Munson, A., Nati, J. J. H., Papatheodoulou, M., & McKenzie, D. J. (2021). Guidelines for reporting methods to estimate metabolic rates by aquatic intermittent-flow respirometry. *Journal of Experimental Biology*, 224, jeb242522. <https://doi.org/10.1242/jeb.242522>
- Klein, S. G., Steckbauer, A., & Duarte, C. M. (2020). Defining CO<sub>2</sub> and O<sub>2</sub> syndromes of marine biomes in the Anthropocene. *Global Change Biology*, 26, 355–363. <https://doi.org/10.1111/gcb.14879>
- Kühl, M., Cohen, Y., Dalsgaard, T., Jorgensen, B. B., & Revsbech, N. P. (1995). Microenvironment and photosynthesis of zooxanthellae in scleractinian corals studied with microsensors for O<sub>2</sub>, pH and light. *Marine Ecology-Progress Series*, 117, 159–172. <https://doi.org/10.3354/meps117159>
- Levin, L. A., & Breitbart, D. L. (2015). Linking coasts and seas to address ocean deoxygenation. *Nature Climate Change*, 5, 401–403. <https://doi.org/10.1038/nclimate2595>
- Linsmayer, L. B., Deheyn, D. D., Tomanek, L., & Tresguerres, M. (2020). Dynamic regulation of coral energy metabolism throughout the diel cycle. *Scientific Reports*, 10, 19881. <https://doi.org/10.1038/s41598-020-76828-2>
- McKeon, C. S., & Moore, J. M. (2014). Species and size diversity in protective services offered by coral guard-crabs. *PeerJ*, 2, e574. <https://doi.org/10.7717/peerj.574>
- Murphy, J. W. A., & Richmond, R. H. (2016). Changes to coral health and metabolic activity under oxygen deprivation. *PeerJ*, 2016, e1956. <https://doi.org/10.7717/PEERJ.1956/SUPP-1>
- Nelson, H. R., & Altieri, A. H. (2019). Oxygen: The universal currency on coral reefs. *Coral Reefs*, 38, 177–198. <https://doi.org/10.1007/s00338-019-01765-0>
- Nielsen, J. J. V., Matthews, G., Frith, K. R., Harrison, H. B., Marzoni, M. R., Slaughter, K. L., Suggett, D. J., & Bay, L. K. (2022). Experimental considerations of acute heat stress assays to quantify coral thermal tolerance. *Scientific Reports*, 12, 16831. <https://doi.org/10.1038/s41598-022-20138-2>
- Nilsson, G. E., & Östlund-Nilsson, S. (2005). Hypoxia tolerance in coral reef fishes. *Fish Physiology*, 2, 583–596. [https://doi.org/10.1016/S1546-5098\(05\)21012-9](https://doi.org/10.1016/S1546-5098(05)21012-9)
- Pacherres, C. O., Ahmerkamp, S., Koren, K., Richter, C., & Holtappels, M. (2022). Ciliary flows in corals ventilate target areas of high photosynthetic oxygen production. *Current Biology*, 32, 4150–4158.e3. <https://doi.org/10.1016/j.cub.2022.07.071>
- Pezner, A. K., Courtney, T. A., Barkley, H. C., Chou, W.-C., Chu, H.-C., Clements, S. M., Cyronak, T., DeGrandpre, M. D., Kekuewa, S. A. H., Kline, D. I., Liang, Y.-B., Martz, T. R., Mitarai, S., Page, H. N., Rintoul, M. S., Smith, J. E., Soong, K., Takeshita, Y., Tresguerres, M., ... Andersson, A. J. (2023). Increasing hypoxia on global coral reefs under ocean warming. *Nature Climate Change*, 13, 403–409. <https://doi.org/10.1038/s41558-023-01619-2>
- Pontes, E., Langdon, C., & Al-Horani, F. A. (2023). Caribbean scleractinian corals exhibit highly variable tolerances to acute hypoxia. *Frontiers in Marine Science*, 10, 861. <https://doi.org/10.3389/FMARS.2023.1120262>
- R Core Team. (2021). *R: A language and environment for statistical computing*. R Foundation for Statistical Computing.
- Rabalais, N. N., Turner, R. E., & Wiseman, W. J., Jr. (2001). Hypoxia in the Gulf of Mexico. *Journal of Environmental Quality*, 30, 320–329. <https://doi.org/10.2134/jeq2001.302320x>
- Regan, M. D., Mandic, M., Dhillon, R. S., Lau, G. Y., Farrell, A. P., Schulte, P. M., Seibel, B. A., Speers-Roesch, B., Ultsch, G. R., & Richards, J. G. (2019). Don't throw the fish out with the respirometry water. *Journal of Experimental Biology*, 222, jeb200253. <https://doi.org/10.1242/jeb.200253>
- Ritz, C., Baty, F., Streibig, J. C., & Gerhard, D. (2015). Dose-response analysis using R. *PLoS One*, 10, e0146021. <https://doi.org/10.1371/journal.pone.0146021>
- Roskoski, R. (2015). Michaelis-Menten Kinetics. In S. J. Enna, D. B. Bylund (Eds.), *Reference module in biomedical sciences* (pp. 1–10). Elsevier, ScienceDirect. <https://doi.org/10.1016/B978-0-12-801238-3.05143-6>
- Rutherford, L. D., & Thuesen, E. V. (2005). Metabolic performance and survival of medusae in estuarine hypoxia. *Marine Ecology Progress Series*, 294, 189–200. <https://doi.org/10.3354/meps294189>
- Sampaio, E., Santos, C., Rosa, I. C., Ferreira, V., Pörtner, H.-O., Duarte, C. M., Levin, L. A., & Rosa, R. (2021). Impacts of hypoxic events surpass those of future ocean warming and acidification. *Nature Ecology & Evolution*, 5, 311–321. <https://doi.org/10.1038/s41559-020-01370-3>
- Seibel, B. A., Andres, A., Birk, M. A., Burns, A. L., Shaw, C. T., Timpe, A. W., & Welsh, C. J. (2021). Oxygen supply capacity breathes new life into critical oxygen partial pressure (Pcrit). *Journal of Experimental Biology*, 224, jeb242210. <https://doi.org/10.1242/jeb.242210>
- Shashar, N., Cohen, Y., & Loya, Y. (1993). Extreme diel fluctuations of oxygen in diffusive boundary layers surrounding stony corals. *The Biological Bulletin*, 185, 455–461. <https://doi.org/10.2307/1542485>
- Shashar, N., Kinane, S., Jokiel, P. L., & Patterson, M. R. (1996). Hydromechanical boundary layers over a coral reef. *Journal of Experimental Marine Biology and Ecology*, 199, 17–28. [https://doi.org/10.1016/0022-0981\(95\)00156-5](https://doi.org/10.1016/0022-0981(95)00156-5)
- Shick, J. M. (1990). Diffusion limitation and hyperoxic enhancement of oxygen consumption in zooxanthellate sea anemones, zoanthids, and corals. *The Biological Bulletin*, 179, 148–158. <https://doi.org/10.2307/1541749>
- Steckbauer, A., Duarte, C. M., Carstensen, J., Vaquer-Sunyer, R., & Conley, D. J. (2011). Ecosystem impacts of hypoxia: Thresholds of hypoxia and pathways to recovery. *Environmental Research Letters*, 6, 25003. <https://doi.org/10.1088/1748-9326/6/2/025003>
- Steckbauer, A., Klein, S., & Duarte, C. (2020). Additive impacts of deoxygenation and acidification threaten marine biota. *Global Change Biology*, 26, 5602–5612. <https://doi.org/10.1111/gcb.15252>
- Suggett, D. J., Edmondson, J., Howlett, L., & Camp, E. F. (2020). Coralclip®: A low-cost solution for rapid and targeted out-planting

- of coral at scale. *Restoration Ecology*, 28, 289–296. <https://doi.org/10.1111/REC.13070>
- Tremblay, N., Hünerlage, K., & Werner, T. (2020). Hypoxia tolerance of 10 Euphausiid species in relation to vertical temperature and oxygen gradients. *Frontiers in Physiology*, 11, 248.
- Ultsch, G. R., & Regan, M. D. (2019). The utility and determination of Pcrit in fishes. *Journal of Experimental Biology*, 222, jeb203646. <https://doi.org/10.1242/jeb.203646>
- Vaquier-Sunyer, R., & Duarte, C. M. (2008). Thresholds of hypoxia for marine biodiversity. *Proceedings of the National Academy of Sciences of the United States of America*, 105(40), 15452–15457.
- Wickham, H. (2016). *ggplot2: Elegant graphics for data analysis* (2nd ed.). Springer International Publishing.
- Wickham, H., Averick, M., Bryan, J., Chang, W., McGowan, L., François, R., Grolemund, G., Hayes, A., Henry, L., Hester, J., Kuhn, M., Pedersen, T., Miller, E., Bache, S., Müller, K., Ooms, J., Robinson, D., Seidel, D., Spinu, V., ... Yutani, H. (2019). Welcome to the Tidyverse. *Journal of Open Source Software*, 4, 1686. <https://doi.org/10.21105/joss.01686>
- WillyWeather. (2023). *Opal reef tide times and heights*, QLD. WillyWeather. <https://tides.willyweather.com.au/qld/far-north/opal-reef.html>
- Wood, C. M. (2018). The fallacy of the Pcrit – Are there more useful alternatives? *Journal of Experimental Biology*, 221, jeb163717. <https://doi.org/10.1242/jeb.163717>
- Xie, Y. (2014). knitr: A comprehensive tool for reproducible research in R. In V. Stodden, F. Leisch, & R. D. Peng (Eds.), *Implementing reproducible computational research* (1st ed.). Chapman & Hall, CRC Press.
- Xie, Y. (2015). Dynamic documents with R and Knitr. In B. Raton (Ed.), *The R series* (2nd ed., pp. 1–294). Chapman & Hall, CRC Press.
- Xie, Y. (2021). knitr: A general-purpose package for dynamic report generation in r. In B. Raton (Ed.), *The R series* (pp. 1–216). Chapman & Hall, CRC Press.
- Xie, Y., Allaire, J., & Grolemund, G. (2018). R markdown: The definitive guide. In B. Raton (Ed.), *The R series* (pp. 1–338). Chapman & Hall, CRC Press.
- Xie, Y., Dervieux, C., & Riederer, E. (2020). R markdown cookbook. In B. Raton (Ed.), *The R series* (pp. 1–360). Chapman & Hall, CRC Press.
- Zhang, Y., & Farrell, A. P. (2022). Testing the hypoxia tolerance and hypoxic performance of fishes: A two-tier screening approach. *Frontiers in Marine Science*, 9, 1544. <https://doi.org/10.3389/FMARS.2022.939239>

## SUPPORTING INFORMATION

Additional supporting information can be found online in the Supporting Information section at the end of this article.

**How to cite this article:** Dilernia, N. J., Woodcock, S., Camp, E. F., Hughes, D. J., Kühl, M., & Suggett, D. J. (2024). Intra-colony spatial variance of oxyregulation and hypoxic thresholds for key *Acropora* coral species. *Ecology and Evolution*, 14, e11100. <https://doi.org/10.1002/ece3.11100>